International Journal of Materials Engineering and Technology
Volume 3, Number 2, 2010, Pages 143-153
Published Online: July 23, 2010
This paper is available online at http://pphmj.com/journals/ijmet.htm

APPLICATION OF FUNCTIONAL GRADIENT AL METAL MATRIX COMPOSITE AS A BRAKE ROTOR-FINITE ELEMENT ANALYSIS

HONGWEN ZHANG, ADAM LOUKUS and JOSH LOUKUS

REL Inc
57640 North Eleventh Street
Calumet, MI 49913, U. S. A.
e-mail: honzhang@mtu.edu

Abstract

Temperature rise and the corresponding thermal stress in disk-shape Al metal matrix composite (MMC) rotors and stainless steel rotor are investigated through finite element analysis (FEA). It is observed that the maximum temperature rise in Al MMC rotors is slightly higher than that in the stainless steel rotor. However, the maximum thermal stress in Al MMC rotors is much lower than that in stainless steel rotor. Results from FEA shows that yield may occur at the inner boundary for the homogeneous metal matrix composite (HMMC) rotor. The functional gradient MMC (GMMC) rotor will significantly reduce the thermal stress at the inner boundary by introducing a volume fraction gradient from the inner to the outer boundary, which enhances the reliability of GMMC using as a rotor.

Introduction

Brake components for ground transportation vehicles have been one of the attractive and potential application markets for Al metallic matrix composites (MMCs) in decades because of the combination of the significant weight reduction

Keywords and phrases: metal matrix composite, thermal stress, rotor, finite element analysis.

Communicated by M. Misbahul Amin

Received July 26, 2009; Revised August 25, 2009

and the performance improvement comparing to the traditional iron/steel rotors. Al MMC rotors, having high thermal conductivity, high specific heat, but low density and low heat capacity, may perform quite differently from the traditional iron/steel rotors during operation [1-4]. Thus, the reliability concerns for Al MMC rotors arise due to temperature rise and thermal stress concentration during operation.

Generally, a non-homogeneous thermal load is generated on the rotor disk upon braking. The linear velocities at the outer part of the rotating rotor disk are greater than the velocities at the inner part. This creates the higher energy at the outer part and thus leads to the higher localized temperature rise. This temperature difference results in the thermal stress concentration in the rotor whose coefficient of thermal expansion (CTE) is constant. If the thermal stress is high enough, two harmful effects could appear (i) the rotor disk may warp and lose its integrity upon application and (ii) the fatigue life of the rotor decrease significantly.

Al MMCs, displaying the excellent thermal conductivity as compared with iron and steels, are expected to dissipate the generated heat quickly into the whole disk and thus decrease the thermal inhomogeneity and the thermal stress concentration. However, the total heat capacity of an Al MMC rotor is only around half of the iron/steel rotor with the same geometry because the density of Al MMCs is only $1/3$ of iron/steels although the specific heat of Al MMCs $(\sim 800\mathrm{J}/(\mathrm{kg}\cdot\mathrm{K}))$ is higher than that of iron/steels $(500\mathrm{J}/(\mathrm{kg}\cdot\mathrm{K}))$. As a result, the temperature rise in Al MMC rotors could be higher than that in iron/steel rotors, which arises the concern of the thermal reliability for Al MMC rotors.

Composites with geometry-dependent thermal properties may help to allow the disk to expand and contract without creating the high thermal stress. This technology, called *Functional Reinforcement Gradient* (FRG), involves using reinforcement to form a composition gradient in MMC rotors. The compositional gradient will adjust the thermal properties and the mechanical properties locally, aiming at releasing the thermal load concentration.

The current work is focused on the thermal response of Al-based gradient MMC (GMMC) rotors upon braking through the finite element analysis. As a comparison, thermal response from an Al homogeneous MMC (HMMC) rotor and a stainless steel rotor are also shown in the current work. It is observed that the thermal stress concentration has been significantly released by using Al GMMC rotor. The volume fraction of the reinforced SiC in Al HMMC rotor is uniformly 40%. The volume

fraction of SiC in Al GMMC rotor ranges from 30 to 50% linearly along the radial direction from the inner to the outer boundary.

Model Setup

The following analysis presents the heat generation and dissipation in a single rotor disk for a sport motorcycle during the panic braking and the following release period. As the brakes slow the bike, they transform the kinetic energy into thermal energy, resulting in intense temperature rise in the brake disk and the brake pads. In the analysis, the motorcycle (400kg) initially travels at 90km/h $(v_0 = 25\,\mathrm{m/s})$ when the driver brakes for 2.5 seconds, causing the vehicle's two brake pad squeezing on one rotor disk to slow the bike at an acceleration rate of $10\mathrm{m/s^2}$ $(a_0 = -6\mathrm{m/s^2})$ until a full stop. The wheels are assumed not to skid against the road surface in the whole process.

The analysis models the brake disk as a 3D solid with the rotor geometry shown in Figure 1. The disk has inner diameter D_{in} of 0.188m, outer diameter D_{out} of 0.292m and the thickness D_{thick} of 0.006m. Neglecting drag and other losses, the brakes' retardation power is given by the negative of the time derivative of the bike's kinetic energy:

$$P = -\frac{d}{dt}\left(\frac{mv^2}{2}\right) = -mv\frac{dv}{dt} = -mR^2\omega(t)\alpha. \tag{1}$$

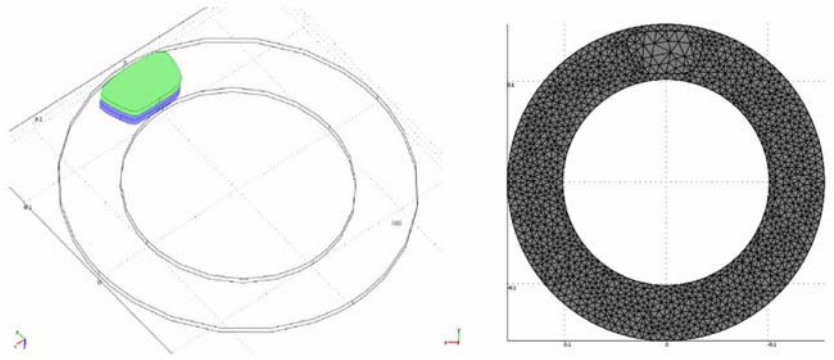

Figure 1. (a) The geometry and the assembly and (b) the mesh of the brake disk and brake pads.

Here, m is the mass of the motorcycle, v the vehicle speed $(v = v_0 + a_0 t)$, R the wheel radius (0.30m), ω the angular velocity $\left(\omega = \omega_0 + \alpha t \text{ and } \omega_0 = \frac{v_0}{R}\right)$ and α the angular acceleration $\left(\alpha = \frac{a_0}{R}\right)$.

The friction force between the pads and the disks provides the source for the retardation, which is acting on the interfaces between pads and disk. The friction force per unit area, f_f is assumed to be approximately a constant over the surface of a single brake pad and is directed opposite to the disk velocity vector (v) [5], which can be written as

$$f_f = -\frac{mR^2\alpha}{2r_p A}, \tag{2}$$

where r_p is the distance from the center of the disk to the pad's center of mass $(r_p = 0.122\text{m})$ and the pad area $A = 0.003\text{m}^2$.

Because it is assumed that the retardation is due entirely to the friction in the brakes, the heat power generated per unit contact area at time t and the distance r from the center becomes

$$q(r, t) = -f_f \cdot v = -\frac{mR^2\alpha}{2r_p A} r(\omega_0 + \alpha t). \tag{3}$$

The heat produced at the interface between the brake pads and the disk is dissipated into both the pads and the disk by conduction. This can be expressed through transient heat transfer equation

$$\rho C_p \frac{\partial T}{\partial t} + \nabla \cdot (-k\nabla T) = -\rho C_p u \cdot \nabla T. \tag{4}$$

In equation (4), k represents the thermal conductivity $(\text{W}/(\text{m} \cdot \text{K}))$ and C_p is the specific heat capacity $(\text{J}/(\text{kg} \cdot \text{K}))$. Moreover, the heat release from the disk and the pad surfaces to the ambient environment is described by both convection and radiation

$$q_{dis} = -h(T - T_{air}) - \varepsilon\sigma(T^4 - T_{air}^4). \tag{5}$$

In this equation, ε is the material's emissivity and σ is the Stefan-Boltzmann constant $(\sigma = 5.67 \cdot 10^{-8}(\mathrm{W}/(\mathrm{m}^2 \cdot \mathrm{K})))$. h equals to the convective film coefficient $(\mathrm{W}/(\mathrm{m}^2 \cdot \mathrm{K}))$, which is a function of the vehicle speed in equation (6) [6]

$$h = \frac{0.027k}{D_{out}}\left(\frac{\rho D_{out} v}{\mu}\right)^{0.8}\left(\frac{C_p \mu}{k}\right)^{0.33}, \tag{6}$$

where μ is the viscosity of air $(\mu = 1.8 \cdot 10^{-5}\mathrm{Pa} \cdot \mathrm{s})$. The properties of rotor materials are shown in Table 1. Some properties of MMC rotor are obtained from a hybrid preform reinforced Al MMCs [7] made by REL Inc. and others are obtained from the properties of the constitutive elements (in Table 1) based on the rule of mixture.

Table 1. Selected physical, thermal and mechanical properties of A319 Al alloy, SiC particle, stainless steel, brake pad and air

	A319	SiC	Stainless steel	Pad	Air
Coefficient of thermal expansion α $(10^{-6}/\mathrm{K})$	22.9	4.5	17.8	-	-
Specific heat Cp $(\mathrm{J/kg/K})$	960	670	500	935	1100
Density ρ $(\mathrm{kg}/\mathrm{m}^3)$	2790	3210	7800	2000	1.17
Thermal conductivity k $(\mathrm{W/m/K})$	110	125	16.2	8.7	0.026
Modulus E (GPa)	73.8	480	200	-	-
Strength σ (MPa)	240	3900	500	-	-
Emissivity e	0.25	0.87	0.28	0.8	-

Results and Discussion

Temperature rise

Figure 2 reveals the temperature contour on the surface of Al GMMC rotor at a braking time of $t = 1.8\mathrm{s}$. It is noted that the hottest area (hot ring) on the surface is located in the middle area which the pad swept over. This observation indicates that the heat is generated and concentrated on the contacting area between the brake pad

and the rotor. At the inner and outer boundary of the rotor, the temperature is low. Thus, a temperature gradient along the radial direction from the hot ring in the middle to the inner or outer boundaries of the rotor is created. Intuitively, the steepest temperature gradient is formed along the 'hot line', shown in Figure 2, which crosses the highest temperature rise spot in radial direction. Consequently, the 'hot line' also represents the largest thermal stress concentration and the investigations are focused on the 'hot line'.

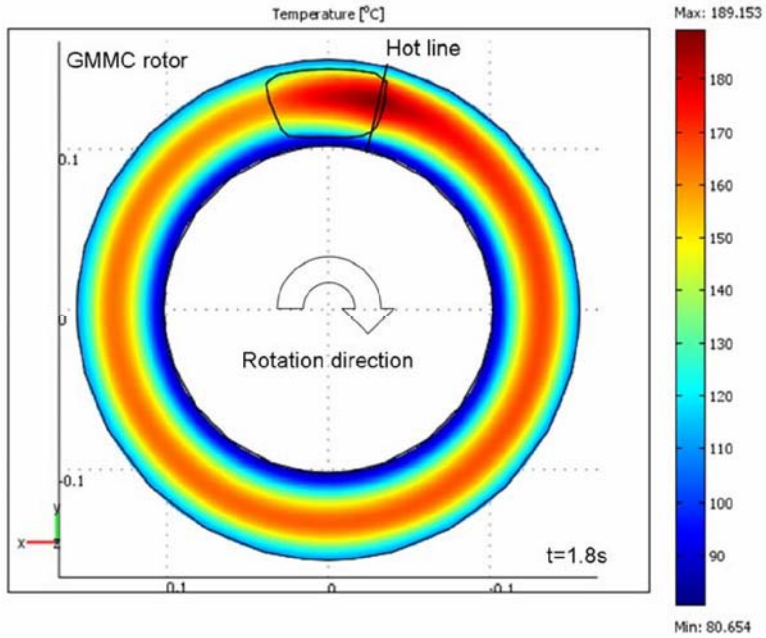

Figure 2. Temperature contour on the surface of a homogeneous MMC rotor at $t = 1.8s$.

Temperature profiles for a GMMC rotor at different braking time along the 'hot line' are shown in Figure 3. At $t = 0.1$s, a temperature plateau is observed, which is in accordance with the area the brake pad swept across. At either boundary of the plateau, steep temperature gradients are seen. With increasing time, the peak temperature increases until the braking time $t = 1.8$s. Within the duration $t \leq 1.8$s, the heat generation rate is higher than the heat dissipation rate due to the high vehicle speed at the early braking stage. Thus, the temperature continuously increases until reaching the maximum temperature $T_{\max} =\sim 190^{\circ}$C. When $t > 1.8$s, the heat generation rate becomes smaller than the heat dissipation rate due to the

slow vehicle speed. When the vehicle completely stops $(t \geq 2.5\text{s})$, no heat is generated afterwards. In the period of $t > 1.8\text{s}$, the peak temperature decreases continuously until a homogeneous temperature is reached in the whole rotor as shown in Figure 3. Then, the temperature of the whole rotor decreases slowly due to the heat dissipation into the ambient environment.

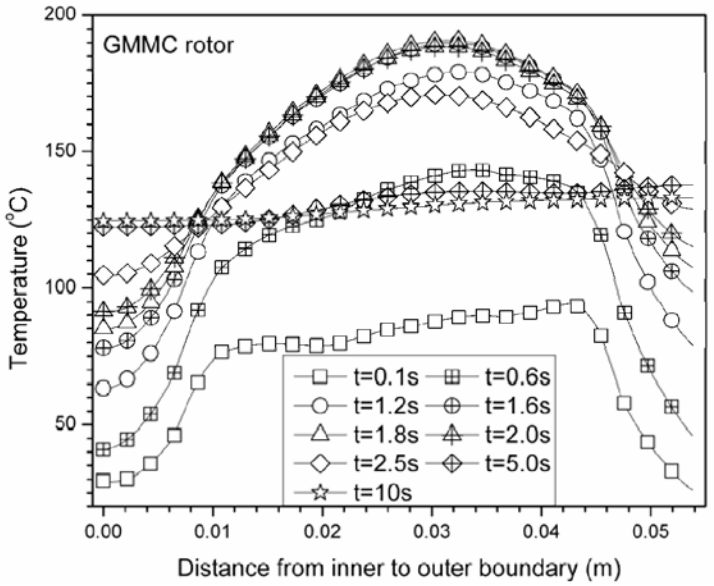

Figure 3. Temperature profiles along the 'hot line' (marked in Figure 2) at different braking time in a GMMC rotor.

The temperature rise in GMMC, HMMC and stainless steel rotors along the 'hot line' at different braking time are shown in Figure 4 for comparison. It is noted that the temperature rise in both GMMC and HMMC rotors during braking are nearly same. The close composition and the similar thermal properties for Al matrix alloy and SiC particles may account for the similar temperature profile during braking. Also, the similar trend of the temperature rise in all three rotors has been observed although the peak temperature in stainless steel is lower than others. The larger heat capacity of the stainless steel accounts for that. Although the higher peak temperature in MMC rotors has been observed in current simulation, a steeper temperature gradient in the stainless steel rotor is obtained. The small thermal conductivity in stainless steel is responsible for the higher temperature gradient because the heat generated cannot be conducted away to the neighboring materials

as quickly as in Al MMC rotors. Moreover, large thermal conductivity in MMCs causes the temperature homogenized quickly along the 'hot line'. At $t = 5\text{s}$, the temperature in MMCs are almost homogeneous while an obvious temperature gradient is still existed in stainless steel rotor, shown in Figure 4.

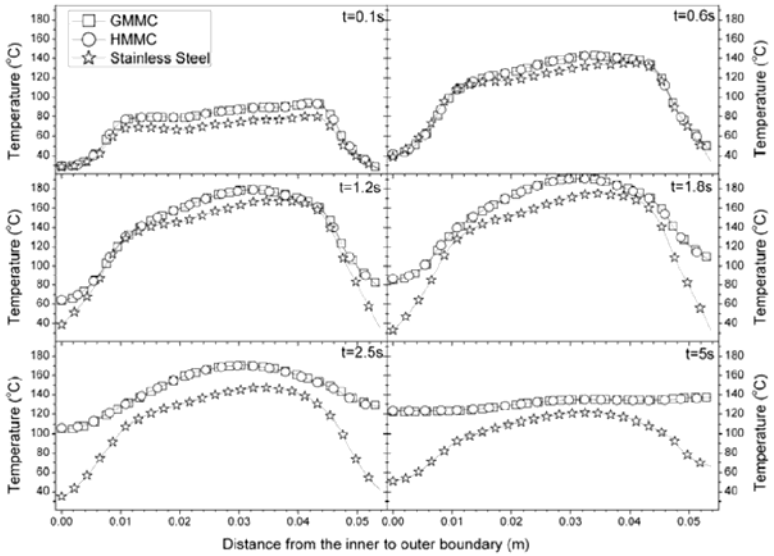

Figure 4. Temperature rise along the 'hot line' in GMMC, HMMC and stainless steel rotors at different braking time.

Thermal stress

Thermal stress (von Mises stress) along the 'hot line' for all three rotors at different braking time is shown in Figure 5. At early stage $(t = 0.1\text{s})$, the thermal stress profiles for all three rotors are similar although the maximum stress in the middle of stainless steel rotor is slightly higher. The thermal stress peaks in the middle of the 'hot line' for all three rotors locate at the contacting area between the pad and the rotor. With increasing time, the higher thermal stress for the stainless steel has distinguished itself clearly from the MMC rotors in Figure 5. At $t = 0.6\text{s}$, two thermal stress valleys in the thermal stress profile of MMC rotors are observed while the valley is hardly found in stainless steel rotor. At $t > 1.2\text{s}$, the stress valleys can be observed for all three rotors in Figure 5. At $t = 1.2\text{s}$, the thermal stresses for all three rotor is comparable at both inner and outer boundaries. At $t = 1.8\text{s}$, the boundary thermal stress in all three rotor increases to beyond the thermal stress in

the middle part. At $t > 1.8\text{s}$ both the boundary and the middle thermal stresses for stainless steel rotor are higher than that in MMC rotors. Also, the thermal stress decrease in all three rotors start to decrease after $t = 1.8\text{s},$ which corresponds to start of temperature homogenization. It is noted that the thermal stress for MMC rotors decrease much quickly than stainless steel rotor in Figure 5. At $t = 5\text{s},$ the maximum thermal stress in MMCs is less than $1/3$ of that in stainless steel rotor. Based on above observation, it is concluded that the thermal stress in MMC rotors is smaller than that in stainless steel rotor.

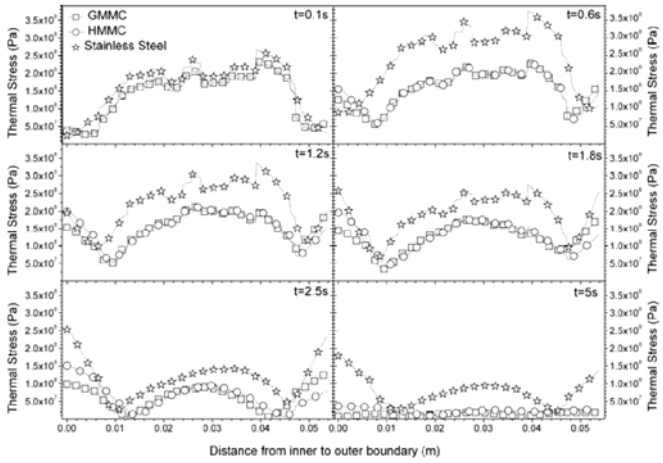

Figure 5. Thermal stress profiles along the 'hot line' in GMMC, HMMC and stainless steel rotor at different brake time.

Moreover, it is noted that introduction of the compositional gradient Al GMMC rotors significantly reduces the thermal stress at the inner boundary of the rotor, which is even smaller than the yield strength of the matrix alloys (A319). This enhances the reliability of the MMC rotor. The lower volume fraction of reinforcement around the inner boundary dramatically decreases the modulus of the composite locally. Thus, the lower thermal stress in the inner boundary of the MMC rotor is achieved.

Coupled thermal and mechanical stress

Beside the thermal stress, the mechanical load also need to be considered for designing a reliable rotor. Friction force (equation (2)) and squeezing force (associated with the friction force by the friction coefficient) are applied on the rotor

through the brake pads. The coupled mechanical and thermal stress profile is calculated along the 'hot line'. The combined stress profile along the 'hot line' shown in Figure 6 is in a similar trend to the thermal stress. The combined stress at the inner boundary is about 25-30% higher than the thermal stress itself although the combined stress in the middle of the rotor shows little enhancement. At duration $1.2\text{s} < t < 1.8\text{s}$, the combined stress at the inner boundary for Al HMMC rotor is around 250MPa, which is higher than the yield strength of the matrix alloy (A319). This will cause the failure of the rotor upon braking. However, for Al GMMC rotor, the stress at the inner boundary is around 200MPa, which is still lower than the yield strength of the matrix alloys. This is indeed the beneficiary of Al GMMC rotor outcoming Al HMMC rotors.

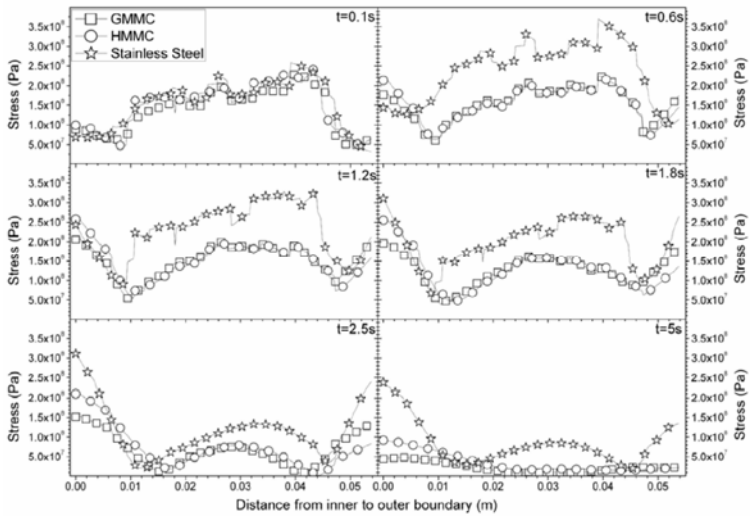

Figure 6. The coupled mechanical and thermal stress along the 'hot line' in GMMC, HMMC and stainless steel rotor at different brake time.

In addition to modify the composite design, the optimization of the brake system, i.e., adjusting the geometry and the dimension of both the pad and the rotor disk, as well as the relative position between the brake pads and the rotor disk can also alter the behavior of the rotors. Thus, to substitute the traditional stainless steel rotors with the Al MMC rotors, a complete and systematic investigation of thermal and mechanical response from the brake system is necessary and more study is still in progress.

Conclusions

Thermal response, including the temperature rise and the thermal stress, in Al MMC and stainless steel rotors was investigated through finite element analysis. The maximum temperature rise in MMC rotor is slightly higher than that in the stainless steel rotor. However, the high thermal conductivity of Al MMC rotor leads to a smaller thermal stress as compared with the stainless steel rotor. The coupled mechanical and thermal stress analysis shows that Al GMMC rotor will significantly decrease the stress at the inner boundary, where yield may occur for Al HMMC rotor.

References

[1] R. Asthana, Journal of Materials Science 33 (1998), 1679-1698.

[2] J. M. Coulson and J. F. Richardson, Chemical Engineering, Vol. 1, Eq. 9.88.

[3] Heat generation in a disk brake in Comsol Multiphysics 3.3A.

[4] http://www.relinc.net/products/lightweight_composite_brakes.

[5] D. B. Miracle, Composites Science and Technology 65 (2005), 2526-2540.

[6] J. S. Moya, S. Lopez-Esteban and C. Pecharroman, Progress in Materials Science 52 (2007), 1017-90.

[7] S. Rawal, JOM 53(4) (2001), 14-17.